Available Online at http://www.journalajst.com

ASIAN JOURNAL OF SCIENCE AND TECHNOLOGY

ISSN: 0976-3376

Asian Journal of Science and Technology
Vol. 11, Issue, 06, pp.11015-11022, June, 2020

RESEARCH ARTICLE

SPECTROSCOPIC STUDIES ON DNA BINDING ABILITY OF FEW RUTHENIUM COMPLEXES AND ANALYSIS OF ANTIMICROBIAL PROPERTIES

[1]Kalita, R.M., [2]Devi, S.P. and [1,*]Medhi, C.

[1]Department of Chemistry, Gauhati University, P.O Gauhati University, Guwahati-781014, Assam, India
[2]Department of Botany, Gauhati University, P.O Gauhati University, Guwahati-781014, Assam, India

ARTICLE INFO

Article History:
Received 07th March, 2020
Received in revised form
19th April, 2020
Accepted 14th May, 2020
Published online 30th June, 2020

ABSTRACT

Few Ruthenium complexes were synthesized. The structures of these complexes are characterized from XRD and spectroscopic techniques. Furthermore computational technique was used to complement the experimental structures. Three complexes were synthesized and assessed the structures of these. UV-visible titration experiment showed the binding of these complexes with CT-DNA. Antimicrobial activity of these complexes was also studies, but Ru-AT and Ru-ANP complexes are found to be good activity and Ru-ATDM complex showed no activity.

Key words:

Trichlorobis (2-acetamidothiazole)ruthenium(III) hydrate (Ru-AT), trichlorobis (2-acetamido-5-nitropyridine) dimethyl sulfoxideruthenium (III) (Ru-ANP), trichlorobis (2-acetamido thiazole) dimethyl sulfoxideruthenium (III) (Ru-ATDM), DFT method, single crystal XRD.

Citation: Kalita, R.M., Devi, S.P. and Medhi. C. 2020. "Spectroscopic studies on DNA binding ability of few Ruthenium complexes and analysis of antimicrobial properties.", *Asian Journal of Science and Technology*, 11, (06), 11015-11022.

INTRODUCTION

Ruthenium(II)/(III) complexes have gained enormous attraction in pharmaceutical and drug discovery due to their biological importance. Several ligands having good biological property are generally used in the synthesis of ruthenium complexes. Here, NAMI-A and KP1019/KP1339 are cited as recent potential anticancer complexes which are under clinical trials [Rosenberg, 1965; Clarke, 1999; Morris, 2001; Kostova, 2006]. Various ruthenium complexes with aromatic ligands like thiazole and pyridine have been synthesized due to interesting biological activity of these ligands. There are extensive studies on the incorporation of these ligands in potential anticancer agents, and synthesis of ruthenium complexes with these ligands are the interest of the present study [Clarke, 2003; Siddiqui, 2009]. The structures of thiazoles are similar to imidazoles and also may have acitivity against diseased cells like many biologically active molecules such as Sulfathiazole(antimicrobial drug), Ritonavir (antiretroviral drug), Abafungin (antifungal drug), Bleomycine and Tiazofurin (antineoplastic drug) [Siddiqui, 2009]. Some ruthenium complexes offer a potential role as antitumor agents over platinum (II) complexes, which are in currently clinical trials, with the properties of a novel mechanism of action, the prospect of non-cross-resistance, reduced toxicity and a different spectrum of activity [Hong-Ke, 2011; Murali, 2002; Sun, 2009; Yang, 2011 ; Rillema, 1982]. may be active anticancer compound, but sometimes low solubility in water is another disadvantage. In fact, the solubility may be related to the incorporation of DMSO molecules as ligand in ruthenium complexes. Quite a few Dimethyl sulfoxide (DMSO) complexes of both Ru(II) and Ru(III) are found as good as cisplatin in terms of anticancer activity [Christian, 2008; Feyer, 2010; Chandra, 2004; Karabasannavar, 2017; Li, 2013; Gray, 2003]. We have synthesized few ruthenium complexes using some known biologically active ligands. Ruthenium is an important metal in inorganic and organometallic chemistry and also less toxic than platinum complexes. We have chosen 2-acetamidothiazole (AT), 2-acetamido-5-nitropyridine (ANP), Dimethyl sulfoxide (DMSO) ligand in the synthesis of few ruthenium complexes.

Experimental section

MATERIALS

Analytical grade $RuCl_3.3H_2O$ was purchased from Sigma, and used without purification.2-acetamidothiazole,2-acetamido-5-nitro pyridine and solvents are used in the synthesis as received.

Preparation

Synthesis of trichlorobis(2 acetamidothiazole) ruthenium (III) hydrate (Ru-AT) complex:

0.1g $RuCl_3.3H_2O$ was refluxed with 3 ml ethanol and 3 ml 1 N HCl for 1 hr. 2 acetamidothiazole ligand (in the ratio 1:2) was dissolved in 1 ml ethanol and 1 ml 5 M HCl was added to refluxing solution after cooling. The mixture was stirred for 1 hr and refluxed at 50°C for half an hour. After cooling at room temperature formation of red crystals were seen and it was again recrystallized from the solvent mixture of dichloromethane and ethanol.

Synthesis of trichlorobis(2 acetamidothiazole) dimethylsulfoxideruthenium (III) (Ru-ATDM) complex: 0.1g $RuCl_3.3H_2O$ was refluxed with mixture of 3 ml ethanol and 3 ml 1N HCl for 1 hr. 2 acetamidothiazole ligand (in the ratio 1:1) was dissolved in 1 ml ethanol and 1 ml 5 M HCl was added to refluxing solution on cooling and stirred for half an hour after adding 0.5 ml DMSO. The solution was stirred for 1 hr and again refluxed at 50°C for 1 hr. On gradual cooling at room temperature red crystals were formed. The crystals were recrystallised from the solvent mixture of acetonitrile and methanol.

Synthesis of trichlorobis (2acetamido-5-nitro pyridine) dimethylsulfoxideruthenium (III) (Ru-ANP) complex: 0.1 g $RuCl_3.3H_2O$ was dissolved in 10 ml ethanol and 1 ml 5N HCl solution and refluxed with for 1 hr. 2 acetamido5 nitro pyridine ligand (in the ratio 1:1) was dissolved in 1 ml ethanol and 2 ml 5 M HCl by slow heating and added to the refluxing solution on subsequent cooling. Again the solution was refluxed for one hr and then 0.5 ml DMSO was added after cooling the solution. The solution was again refluxed at 50°C for 1 hr. Orange crystals were observed and recrystallized from the solvent mixture of acetonitrile and methanol.

Characterization of complexes: The IR spectra of the complex were recorded as KBr pellets on a Shimadzu IR Affinity-1 Perkin-Elmer FT-IR spectrophotometer. The UV-visible spectra were taken in DMSO solvent in a Shimadzu UV-2401 PC spectrophotometer.

Crystallography of complexes: Fine crystals were mounted on glass capillary and single crystal X-Ray diffraction data we recorded at 100 K with Bruker smart AXS diffractometer with graphite-monochromatised Mo-Kα radiation by ϕ-ωscans. The molecular graphic structure was analyzed by ORTEP plot program(Figures 1-3). Experimental details are given in Table 1.

Infrared spectra: The IR peaks with tentative assignments (ν_{max}/cm-1) of Ru-AT, Ru-ATDM and Ru-ANP complexes are recorded.

- Ru-AT complex : The IR peaks with tentative assignments (ν_{max}/cm-1) at 3417(NH_2), 2941 (CH_3 of DMSO), 1633(C=O), 833 (C-S,DMSO), 1546 (C=N), 1431(C=C)1224 (C-N), 756 (C-S-C), 596 (Ru-Cl), 516(Ru-N) and 482 (Ru-O) are observed.
- Ru-ATDM complex: The IR peaks with tentative assignments (ν_{max}/cm-1) at 3417(NH_2), 2972 (CH_3 of DMSO), 1639(C=O), 1562 (C=N), 1463(C=C),1298 (C-N), 720 (C-S-C) 1078 (S=O, DMSO), 634 (Ru-Cl), 507(Ru-N) and 472 (Ru-O) are observed.
- Ru-ANP complex : The IR peaks with tentative assignments (ν_{max}/cm-1) at 3444(NH_2), 2966 (CH_3 of DMSO), 1622(C=O), 1519 (C=N), 1422(C=C),1234 (C-N), 720 (C-S-C) 1085(S=O, DMSO), 545(Ru-Cl), 480(Ru-N), 428 (Ru-O) and 1332(Ar-NO_2) are observed.

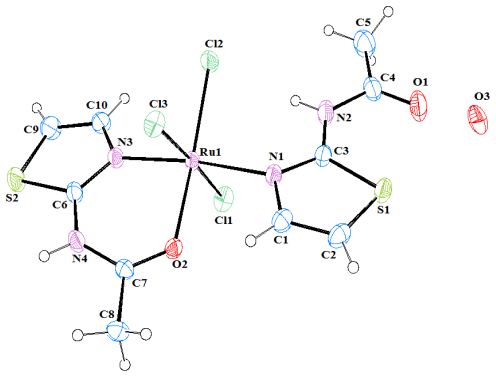

Figure 1. Ortep structure of Ru-AT complex

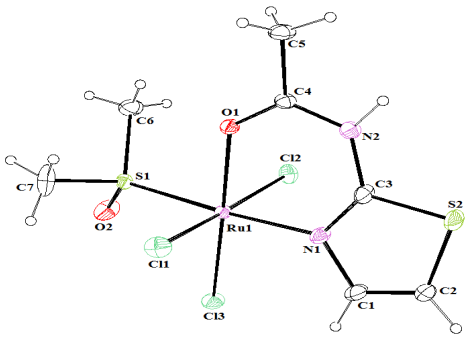

Figure 2: Ortep structure of Ru-ATDM complex

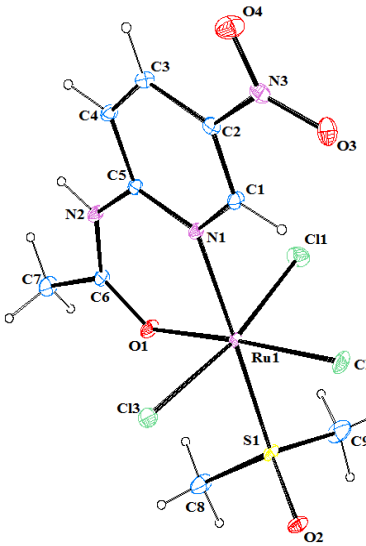

Figure 3. Ortep structure of Ru-ANP complex

UV-visible: The UV-visible absorption spectra of solution of ruthenium complexes in DMSO shows two characteristic peak near visible region. The λmax value of Ru-AT, Ru-ATDM and Ru-ANP complexes are recorded where intraligand π-π* transition for these complexes are observed at 296 nm(Ru-AT), 289(Ru-ATDM) and 292(Ru-ANP).

Table 1: Summary of the crystallographic data of ruthenium complexes.

Parameters	Ru-AT complex	Ru-ATDM complex	Ru-ANP complex
Crystal system	Triclinic	Monoclinic	Monoclinic
Wavelength	0.71073 A^0	0.71073 A^0	0.71073 A^0
Space group	P -1	P 21/c	P 21/c
Empirical formula	C10 H12 Cl3 N4 O3 Ru S2	$C_7H_{12}Cl_3N_2O_2RuS_2$	$C_9H_{13}Cl_3N_3O_4RuS$
Formula weight	507.78	427.73	502.73
Z	2	4	4
Unit cell dimensions	a=7.9009(6) b=9.0476(10) c=13.0619(10) α=80.959(5)^0 β==82.052(4)^0 γ=74.297(3)^0	a=7.0397(4) b=13.2808(10) c=15.7529(9) α=90^0 β==102.772(3)^0 γ=90^0	a=7.7501(2) b=13.7981(3) c=15.7498(4) α=90^0 β==103.426(1)^0 γ=90^0
T(K)	296(2)	296(2)	296(2)
Volume	883.19(14) A_0^3	1436.34(16)A^{03}	1638.20(7)A^{03}
Density	1.909 g/cm^3	1.978 g/cm^3	2.038 g/cm^3
Absorption coefficient	1.593 mm-1	1.930mm-1	1.597mm-1
T_{max},T_{min}	29.146,2.357	29.080,1.325	29.087,1.986
R(reflections)	0.0343(4031)	0.0336(3734)	0.029(4353)
wR2	0.1178	0.0830	0.1037
F(000)	502	844	996
Index ranges	-10<=h<=10 -12<=k<=11 -17<=l<=17	-9<=h<=9 -17<=k<=17 -21<=l<=21	-10<=h<=10 -18<=k<=16 -21<=l<=18
Reflectionscollected	16296	22094	16721
No of parameters	210	190	194
Goodness-of-fit on F2	0.822	1.096	0.848

Weighting scheme
1/[\s^2^(Fo^2^)+(0.1000P)^2^+0.9427P] where P=(Fo^2^+2Fc^2^)/3' (Ru-AT complex)
1/[\s^2^(Fo^2^)+(0.0348P)^2^+1.8325P] where P=(Fo^2^+2Fc^2^)/3'(Ru-ATDM complex)
1/[\s^2^(Fo^2^)+(0.1000P)^2^+0.6768P] where P=(Fo^2^+2Fc^2^)/3'(Ru-ANP complex)

Table 2. Selected bond lengths (Å) and bond angles (°) obtained from crystal structure of Ru-AT complex and the corresponding optimized structures(B3LYP/SDD)

Bond Types	Bond lengths	Angle types	Angles
Ru(1)-Cl(1)	2.334 (2.327)	Cl(2)-Ru(1)-Cl(3)	89.9 (91.5)
Ru(1)-Cl(2)	2.357 (2.331)	Cl(1)-Ru(1)-Cl(3)	176.1 (164.7)
Ru(1)-Cl(3)	2.358 (2.344)	Cl(1)-Ru(1)-Cl(2)	93.8 (95.3)
Ru(1)-O(2)	2.047 (2.044)	N(1)-Ru(1)-Cl(3)	90.6 (86.1))
Ru(1)-N(1)	2.116 (2.118)	N(1)-Ru(1)-Cl(2)	95 (91.5)
Ru(1)-N(3)	2.052 (2.032)	N(1)-Ru(1)-Cl(1)	89.4 (85.6)
C(1)-C(2)	1.342 (1.332)	O(2)-Ru(1)-Cl(3)	86.6 (84.8)
C(1)-N(1)	1.391 (1.381)	O(2)-Ru(1)-Cl(2)	176.4 (163.7)
C(2)-S(1)	1.723 (1.751)	O(2)-Ru(1)-Cl(1)	89.4 (86.8)
C(3)-N(1)	1.322 (1.387)	O(2)-Ru(1)-N(1)	86 (101.1)
C(3)-N(2)	1.362 (1.372)	O(2)-Ru(1)-N(3)	87.6 (82.1)
C(3)-S(1)	1.717 (1.778)	C(2)-C(1)-N(1)	116.2 (115.6)
C(4)-O(1)	1.234 (1.221)	C(1)-C(2)-S(1)	109.7 (113.2)
C(4)-N(2)	1.368 (1.398)	N(1)-C(3)-N(2)	121.8 (127.1)
C(4)-C(5)	1.499 (1.499)	N(1)-C(3)-S(1)	114.6 (112.8)
C(6)-N(3)	1.316 (1.347)	N(2)-C(3)-S(1)	123.4 (120.1)
C(6)-N(4)	1.386 (1.384)	O(1)-C(4)-N(2)	120.1 (116.1)
C(6)-S(2)	1.711 (1.775)	O(1)-C(4)-C(5)	23.9 (131.2)

*Bond lengths and bond angles of optimized structure are given within brackets.

Table 3. Selected bond lengths (Å) and bond angles (°) obtained from crystal structure of Ru-ATDM complex and the corresponding optimized structures(B3LYP/SDD)

Bond Types	Bond lengths	Angle types	Angles
Ru(1)-Cl(1)	2.328 (2.312)	Cl(1)-Ru(1)-Cl(2)	173.5 (171.4)
Ru(1)-Cl(2)	2.356 (2.229)	Cl(3)-Ru(1)-Cl(2)	93.2 (101.3)
Ru(1)-Cl(3)	2.307 (2.220)	Cl(3)-Ru(1)-Cl(1)	92.0 (80.1)
Ru(1)-S(1)	2.296 (2.376)	S(1)-Ru(1)-Cl(2)	90.7 (82.3)
Ru(1)-N(1)	2.092 (1.928)	S(1)-Ru(1)-Cl(1)	92.8 (76.7)
Ru(1)-O(1)	2.060 (1.927)	S(1)-Ru(1)-Cl(3)	90.1 (78.2)
C(1)-N(1)	1.397 (1.302)	N(1)-Ru(1)-Cl(2)	88.2 (99.1)
C(1)-C(2)	1.337 (1.317)	N(1)-Ru(1)-Cl(1)	87.8 (80.7)
C(2)-S(2)	1.684 (1.703)	N(1)-Ru(1)-Cl(3)	93.5 (103.5)
C(3)-N(2)	1.385 (1.302)	N(1)-Ru(1)-S(1)	176.2 (172.5)
C(3)-S(2)	1.724 (1.811)	O(1)-Ru(1)-Cl(2)	86.6 (96.7)
C(4)-O(1)	1.247 (1.286)	O(1)-Ru(1)-S(1)	88.2 (99.2)
C(4)-N(2)	1.337 (1.421)	O(2)-S(1)-Ru(1)	119.1 (166.1)
C(4)-C(5)	1.484 (1.499)	C(4)-N(2)-C(3)	127.7 (114.1)
C(6)-S(1)	1.777 (1.811)	C(1)-C(2)-S(2)	113.4 (120.2)
C(7)-S(1)	1.757 (1.801)	N(1)-C(3)-S(2)	116.5 (110.7)

*Bond lengths and bond angles of optimized structure are given within brackets.

Table 4: Selected bond lengths (Å) and bond angles (°) obtained from crystal structure of Ru-ANP complex and the corresponding optimized structures(B3LYP/SDD)

Bond Types	Bond lengths	Angle types	Angles
Ru(1)-Cl(1)	2.327 (2.329)	Cl(1)-Ru(1)-Cl(3)	170.5 (164.2)
Ru(1)-Cl(2)	2.313 (2.320)	Cl(2)-Ru(1)-Cl(3)	94.0 (96.4)
Ru(1)-Cl(3)	2.335 (2.322)	Cl(2)-Ru(1)-Cl(1)	94.2 (92.4)
Ru(1)-S(1)	2.283 (2.205)	S(1)-Ru(1)-Cl(3)	90.5 (90.2)
Ru(1)-N(1)	2.117 (2.007)	S(1)-Ru(1)-Cl(2)	86.1 (87.2)
Ru(1)-O(1)	2.041 (1.982)	N(1)-Ru(1)-Cl(3)	88.0 (86.8)
C(1)-N(1)	1.348 (1.441)	N(1)-Ru(1)-Cl(2)	94.7 (95.4)
C(1)-C(2)	1.363 (1.338)	N(1)-Ru(1)-S(1)	178.4 (172.4.)
C(2)-N(3)	1.471 (1.502)	O(1)-Ru(1)-Cl(3)	85.5 (86.6)
C(3)-C(4)	1.366 (1.351)	O(1)-Ru(1)-Cl(2)	176.2 (163.7)
C(5)-N(1)	1.351 (1.311)	N(1)-C(1)-C(2)	122.0 (122.2)
C(6)-O(1)	1.238 (1.282)	C(1)-C(2)-C(3)	121.4 (124.6)
C(6)-N(2)	1.335 (1.382)	N(1)-C(5)-C(4)	122.0 (127.9)
C(7)-C(6)	1.486 (1.493)	O(1)-C(6)-N(2)	124.7 (120.6)
C(8)-S(1)	1.760 (1.801)	O(1)-C(6)-C(7)	118.1 (111.9)

*Bond lengths and bond angles of optimized structure are given within brackets.

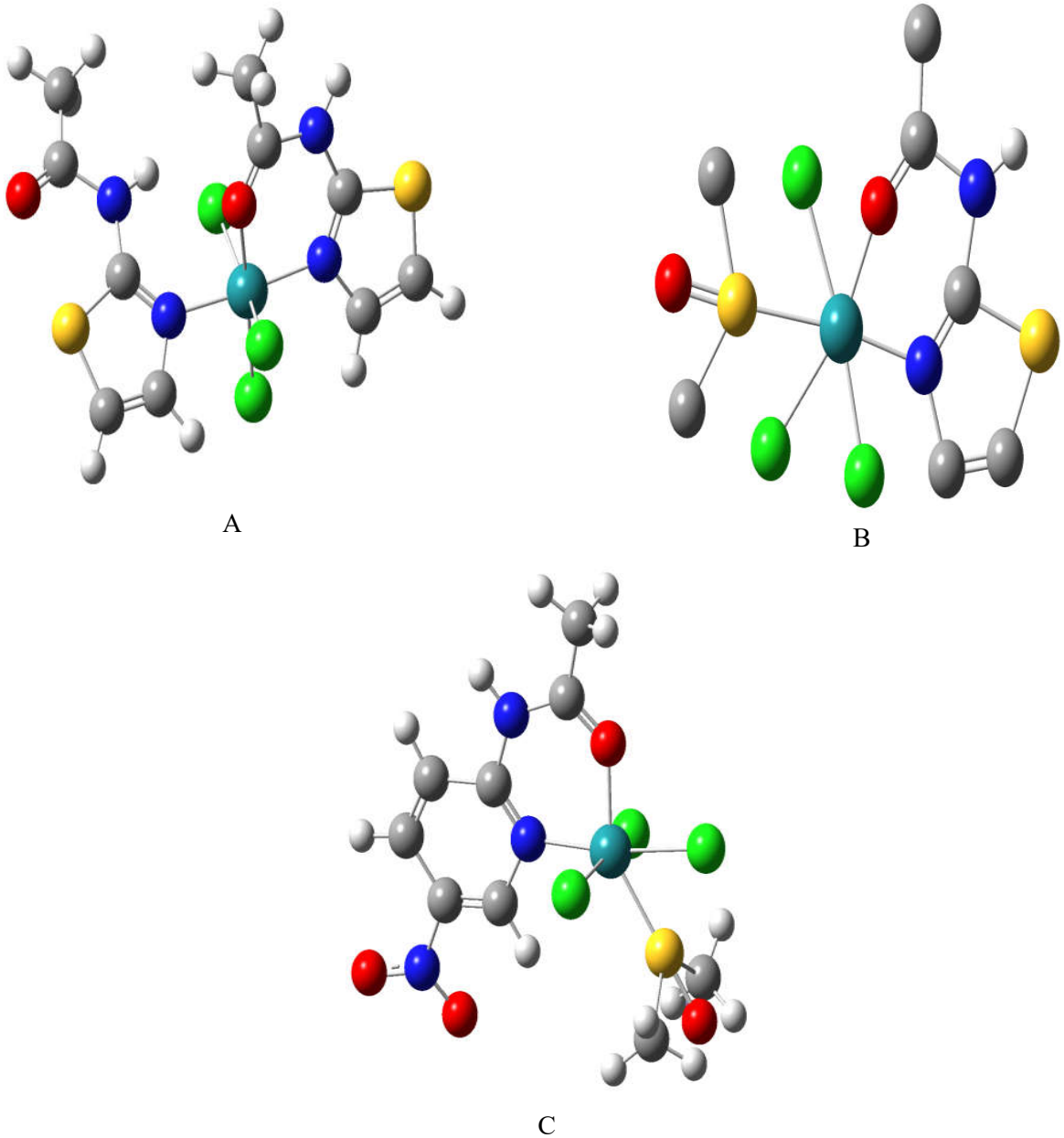

Figure 4: a) trichlorobis(2 acetamidothiazole)ruthenium(III) (Ru-AT) complex. b) Structure of trichlorobis(2 acetamidothiazole)dimethylsulfoxideruthenium(III) (Ru-ATDM) complex. c) Structure of trichlorobis (2 acetamido-5-nitro pyridine) dimethylsulfoxideruthenium (III) (Ru-ANP) complex

Figure 5: Zone of inhibition of Ru-AT complex with negative zone of inhibition of Ru-ANP complex

Table 5. Zone of inihibition of ruthenium complex

Microorganism	Types of microorganism	MCC NO.	Zone of inhibition(mm)	Zone of inhibition(stanrdard mm)
Ru-AT Complex	Staphyloococcus aureus	2408	15	16
	Klebsiella pneumonia	2451	08	10
	Acinetobactes banmani	3083	06	18
	Pseudomonas aeroginesa	2035	16	20
	Candida albicans (Yeast)	1151	14	10
Ru-ANP Complex	Staphyloococcus aureus	2408	-	44
	Klebsiella pneumonia	2451	18	10
	Acinetobactes banmani	3083	07	18
	Pseudomonas aeroginesa	2035	-	16
	Candida albicans (Yeast)	1151	-	10

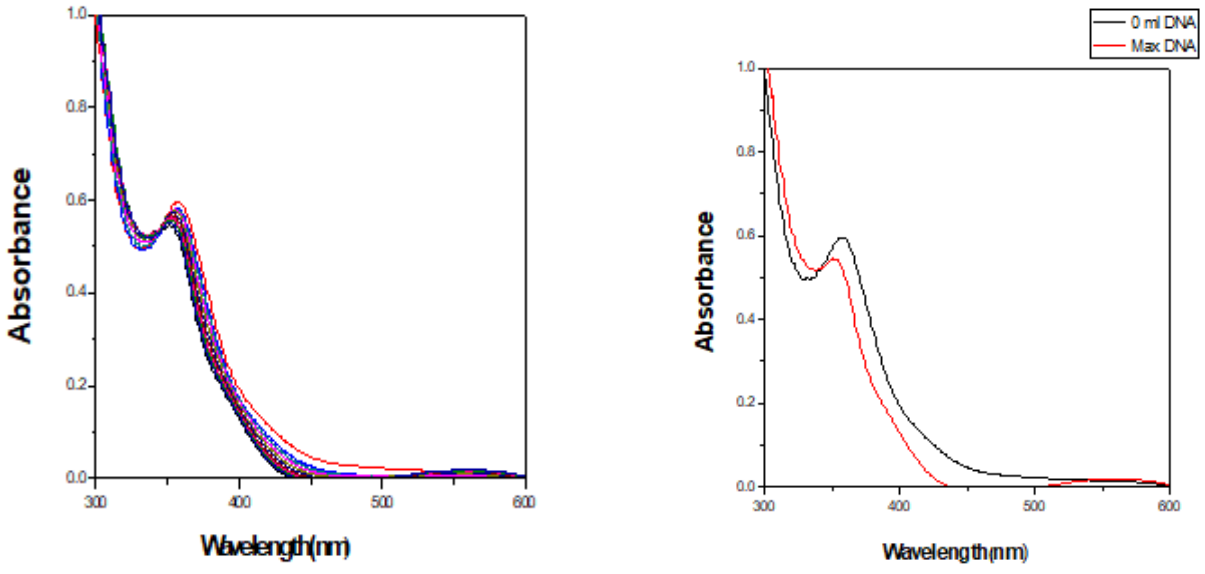

a B

Figure 6: (a) UV-visible spectra of Ru-AT complex inTris-buffer(pH=7.4) with increasing concentration of CT-DNA. (b) λ_{max} shifts from 358 nm to 351 nm(Absorbance decreases on increasing the concentration of DNA)

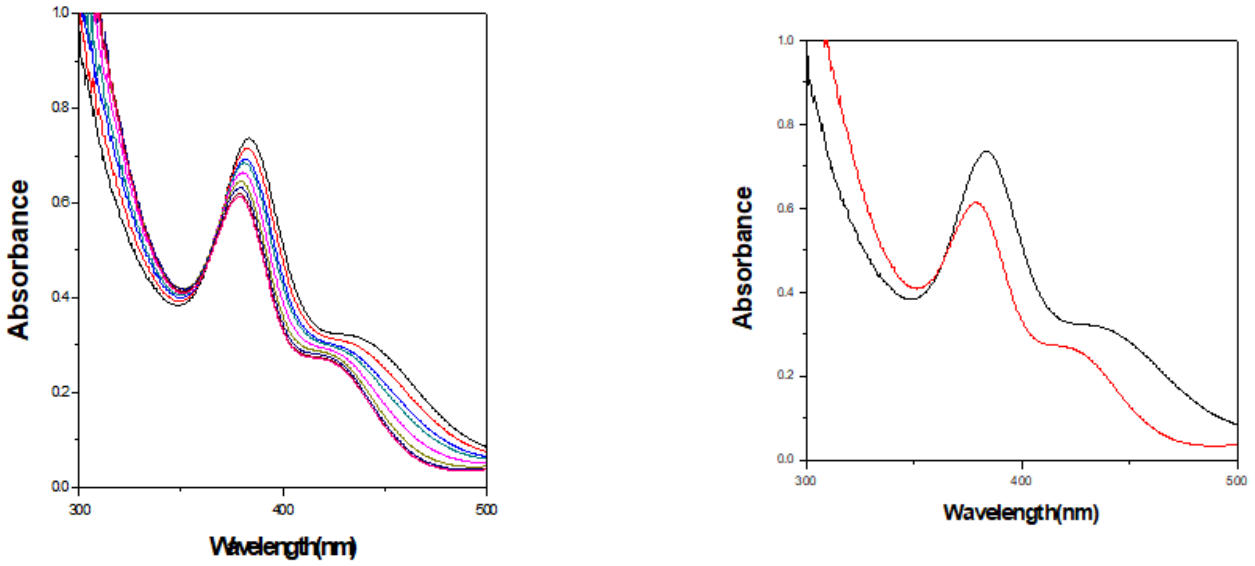

a B

Figure 8: (a) UV-visible spectra of Ru-ANP complex inTris-buffer(pH=7.4) with increasing concentration of CT-DNA. (b) λ_{max} shifts from 378 nm to 375 nm(Absorbance increases on increasing the concentration of DNA)

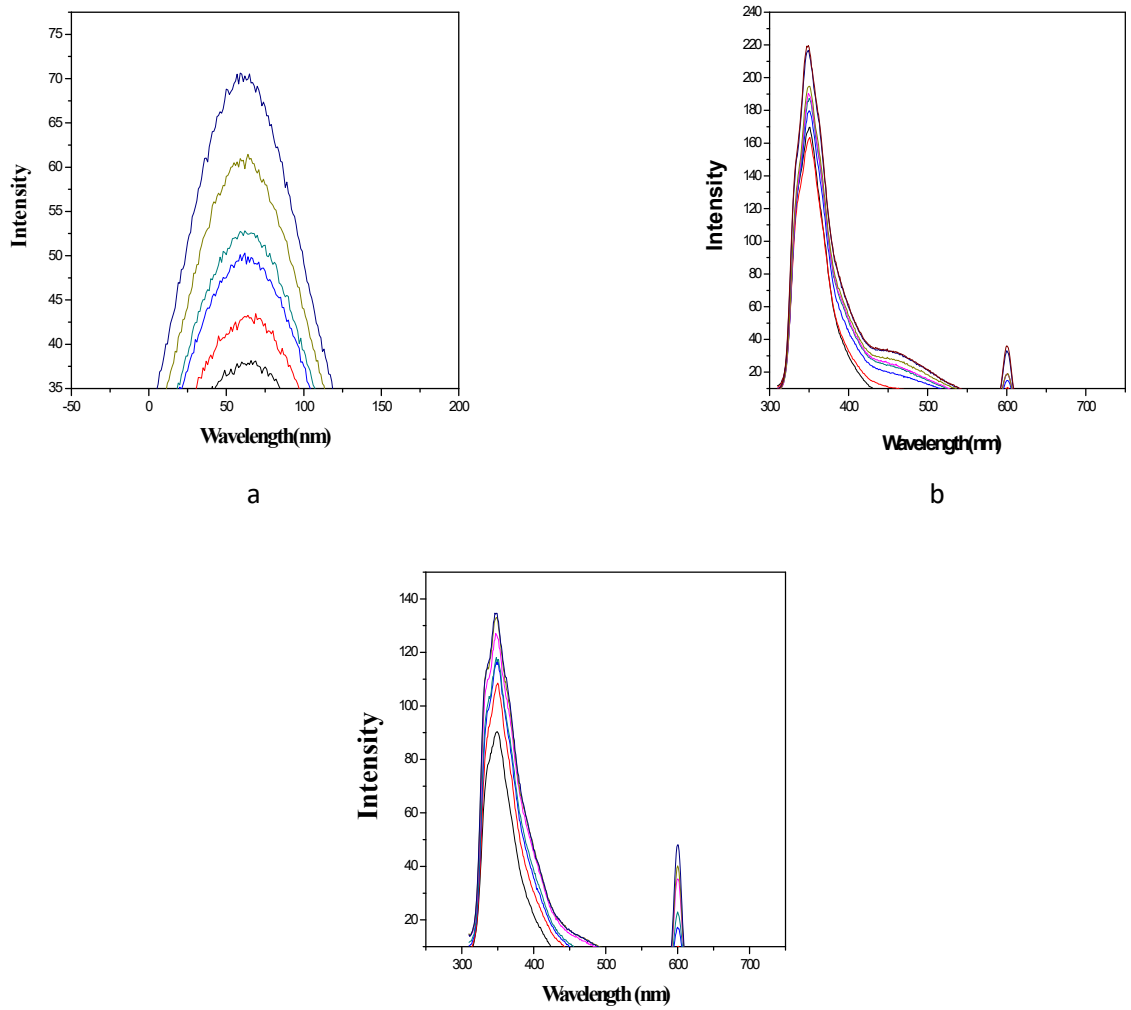

a b c

Figure 9: Fluorescence spectra of (a) Ru-AT complex (Exciting wavelength = 298nm) with different concentrations of CT-DNA (b) Ru-ATDM complex (Exciting wavelength = 300 nm) with different concentrations of CT-DNA. (c) Ru-ANP complex (Exciting wavelength = 300 nm) with different concentrations of CT-DNA

The another peak for LMCT transition are indicated at 358 nm (Ru-AT), 383(Ru-ATDM) and 378 (Ru-ANP) respectively.

CHN Analysis: The percentage of carbon, hydrogen and nitrogen were estimated and compared with the calculated values given in brackets**.**

- For Ru-AT complex are C 24.87(24.43), H 2.43(2.87), N 11.08(11.39).
- For Ru-ATDM complex calc. C 19.96 (19.67), H 2.36 (2.83)%, N 6.17(6.55).
- For Ru-ANP complex calc. C 23.69 (23.17), H 2.40(2.81), N 8.89 (9.03).

Crystallography of Ru-AT, Ru-ATDM and Ru-A **complexes:** Single crystal X-Ray diffraction data were recorded at 100 K with Bruker smart AXS diffractometer with graphite-monochromatised Mo-Kα radiation by ϕ-ω scans. We have used full matrix least square on F^2. The molecular graphic structures of these three complexes were analyzed by ORTEP program. The structures were refined by using SHELXL-97. A summary of the crystallographic data and collections are listed in Table 1. Ruthenium coordinated bond parameters of complexes are given in Tables 2-4 respectively. The crystal structures for the complexes Ru-AT, Ru-ATDM and Ru-ANP are shown in Figures 1, 2 and 3 respectively(Deposition Numbers: 1991691,1991691, 1991694).

Quantum mechanical method of predicting structure of Ruthenium complexes: The geometries are completely optimized B3LYP/SDD method by using Gaussian 03 package(19(a)). The structures of AT, ATDM and ANP complexes are drawn before geometry optimization with Gaussview((19(b))). The optimized structures of complexes are given in figures and the selected bond lengths and angles are given in Tables (2-4) . Moreover, the optimized geometries was utilized to understand the crystal structures of these complexes. In this study, some differences in bond lengths and bond angles of crystal structures from the optimized structure are observed twenty-two diverse compounds were prepared and Determination of the crystal structures of the prepared compounds depend on several factors i.e accumulation of ions and water molecules in the crystal packing, however the gas phase structure is obtained from quantum mechanical calculations. So slight variation in the geometrical parameters is observed, but the structures are similar. The geometries predicted by using B3LYP/SDD are generally acceptable. The theoretically obtained structures are shown in Figures 4(a)-(c).

Antimicrobial activity: Some of the Ruthenium complexes are known for having excellent antimicrobial property and also because of its activity towards drug resistance microorganisms. The bacterial internal structures are protected by cytoplasm membrane which consists of lipid bilayer. Due to permeability barrier through the cell membrane by various substances in both ways i.e. inside and outside the cell acts as regulating such diffusion processes. So compatibility of cell membrane with drug molecule is very essential. Sometimes they may be resistant to variety of drugs. Out of these three complexes only Ru-AT and Ru-ANP display activity (Table 5). Initially antimicrobial activity of Ruthenium complexes were tested against four bacterial strains such as Staphylococcus aureus, Klebsiella pneumonia, Acinetobactes banmani, Pseudomonas aeroginesa and one fungal/yeast strain Candida albicans by agar well diffusion method. Ru-AT complex displayed activity against all the gram positive, gram negative bacteria and yeast. Ru-ANP complex shows significant zone of inhibition against gram negative bacteria(Figure 5). In some cases DMSO will exhibit moderate zone of inhibition. Since all the complexes are dissolved in DMSO in that case zone of inhibition of complexes are calculated by subtracting the zone of inhibition of DMSO.

Spectroscopic studies on DNA binding of Ruthenium complex

UV-Visible Absorption Titration: The measurement of UV absorption of compounds was conducted in the Tris HCl buffer(pH 7.4) By using a fixed concentration of Ru complex , increments of the CT-DNA stock solution was added. The solutions were allowed to incubate for 30 minutes before the absorption spectra were recorded. Shifting of spectra in the visible region at λ_{max} after adding CT- DNA at different concentrations was observed(6(a)-(b)-8(a)-(b)). With the increase of the CT-DNA concentrations, blue shift occurred and the absorbance decreases. The absorption spectra of the complexes have been characterized by the distinct intense transitions in the wavelength, which ranges within 400 nm. These spectral characteristics suggest the possible interaction between the complex and CT-DNA.

Fluorescence emission studies: Fluorescence emission study is performed keeping the concentration of metal complex constant and by adding different concentrations of CT-DNA. Upon addition of CT DNA the emission intensities of this complex have been increased which indicates that complex may interact with CT-DNA. On addition of CT DNA the emission intensities of the complexes are increased that implies strong interaction of the complex with DNA. However, the hydrophobic environment inside the DNA helix may restrict the mobility of the complex towards the binding site, thereby producing binding capability of these complexes. The CT-DNA emits luminescence in tris buffer at room temperature at the maximum emission wavelength of 670 nm. With the increase of the concentrations of complex, the intensity of emission decreases due to the interaction of the complex with CT-DNA(Figures 9(a)-(c)).

Conclusion

We have synthesized three biologically important Ru complexes by using simple synthetic route. The structures are very similar to the theoretically obtained geometries. The DNA binding ability of these complexes are clearly shown from the UV visible and Fluorescence emission studies. The binding of these complexes with DNA is not straight forward. In addition Ru-AT and Ru-ANP complexes are found to be good antimicrobial activity but Ru-ATDM complex does not show any activity.

REFERENCES

Rosenberg, B. L. V. Camp, T. Krigas, 1965. *Nature*, *205*, 698.
Clarke M. J., F. Zhu, Frasca DR. 1999. *Chem Rev., 99,* 2511.
Vessieres A, Top S, Beck W, Hillard E, Jaouen G. 2006. *Dalton Trans 529,* 529.

Morris RE, Aird RE, Mudroch PS, Chen H, Cummins J, Hughes ND, Parsons S, Parkin A, Boyd G, Jodrell D. I., Sadler P. J. 2001. *J Med Chem., 44,* 3616.

Kostova, I. 2006. *Curr Med Chem., 13,* 1085-107.

Clarke M. J. 2003. Coord. *Chem Rev., 236,* 209.

Siddiqui, N., M.F. Arshad, W. Ahsan and M.S. Alam, 2009. *Int. J. Pharm. Sci. Drug Res*. 1 136-143

Hong-Ke Liu, Peter J. 2011. Sadler, *Acc. Chem. Res., 44,* 349-359.

Finlay GJ, Baguley BC, Cancer Chemother Pharmacol., 2000, *45,* 417-22.

Murali, S. C. V.Sastri, B. G. 2002. Maiya, Proc. Indian Acad. Sci. (Chem. Sci.), *114,* 403- 415.

Sun, S., Yang, Y., Liu, F., Fan, J. X. Peng, J. Kehr, L. 2009. Sun, *Dalton Trans., 38,* 7969-7974.

Yang Yong-guang, Liu Du, Xia Yu, Zhou Yan-hui, Zhong Xue-yun, Liu Jie, 2011. *Chem. Res.,* Chinese Universities, , *27,* 345-349

12.D. P. Rillema, K. B. Mack, *Inorg. Chem.,* 1982, *21,* 3849.

Christian G. Hartinge, Michael A. Jakupec, Stefanie Zorbas-Seifried, Michael Groessl, Alexander Egger, Walter Berger, Haralabos Zorbas, 2008. Paul J. Dyson, Bernhard K. Keppler, *Chemistry & Biodiversity (Review), 5,* 2140-2155.

Feyer, V., Plekan, O., Richter, R., Coreno, M., M.de. Simone, K.C. Prince, A.B. Trofimov, I.L. Zaytseva, J. 2010. Schirmer, *J. Phys. Chem., 114*, 10270–10276.

Chandra, A.K., Michalska, D., Wysokinsky, R., Huyskens, T.Z. 2004. *J. Phys. Chem. A., 108* ,9593–9600.

Karabasannavar, S., Allolli, P., Shaikh, N., Kalshetty M. 2017. *J of Pharmaceutical., 51.*

Li, M., Lan, T., Lin. Z. 2013. *J. Inorg. Chem., 18,* 993-1003.

Gray J.J., Moughon S., Wang C., Schueler-Furman O., Kuhlman B., Rohl C.A., Baker D. 2003. "Protein-protein docking with simultaneous optimization of rigid-body displacement and side-chain conformations", *J. Mol. Biol*., 331, 281-299.

(a) Gaussian 03, Revision B.04, M. J. Frisch, G. W. Trucks, H. B. Schlegel, G. E. Scuseria, M. A. Robb, J. R. Cheeseman, J. A. Montgomery, Jr., T. Vreven, K. N. Kudin, J. C. Burant, J. M. Millam, S. S. Iyengar, J. Tomasi, V. Barone, B. Mennucci, M. Cossi, G. Scalmani, N. Rega, G. A. Petersson, H. Nakatsuji, M. Hada, M. Ehara, K. Toyota, R. Fukuda, J. Hasegawa, M. Ishida, T. Nakajima, Y. Honda, O. Kitao, H. Nakai, M. Klene, X. Li, J. E. Knox, H. P. Hratchian, J. B. Cross, C. Adamo, J. Jaramillo, R. Gomperts, R. E. Stratmann, O. Yazyev, A. J. Austin, R. Cammi, C. Pomelli, J. W. Ochterski, P. Y. Ayala, K. Morokuma, G. A. Voth, P. Salvador, J. J. Dannenberg, V. G. Zakrzewski, S. Dapprich, A. D. Daniels, M. C. Strain, O. Farkas, D. K. Malick, A. D. Rabuck, K. Raghavachari, J. B. Foresman, J. V. Ortiz, Q. Cui, A. G. Baboul, S. Clifford, J. Cioslowski, B. B. Stefanov, G. Liu, A. Liashenko, P. Piskorz, I. Komaromi, R. L. Martin, D. J. Fox, T. Keith, M. A. Al-Laham, C. Y. Peng, A. Nanayakkara, M. Challacombe, P. M. W. Gill, B. Johnson, W. Chen, M. W. Wong, C. Gonzalez, and J. A. Pople, Gaussian, Inc., Pittsburgh PA, 2003. 2. GaussView 3.0, Gaussian, Inc., Pittsburgh PA, 2003.

(b) Gaussview, 2003.

****